Technical note: Assessing pretreatment approaches for ~~sedimentary organic carbon prior to~~ serial pyrolysis-oxidation analysis of sedimentary organic carbon~~Acidification methodology impacts sediment decarbonation as revealed by bulk and serial oxidation measurements~~

Songfan He[1], Huiyuan Yang[1], Xingqian Cui[1]

[1]School of Oceanography, Shanghai Jiao Tong University, Shanghai, 200030, China

Correspondence to: Xingqian Cui (cuixingqian@sjtu.edu.cn) or Huiyuan Yang (yhy_0707@sjtu.edu.cn)

Abstract. ~~Acidification is frequently adopted to remove carbonates preceding particulate organic carbon (POC) measurements. In practice, a~~The ramped-temperature pyrolysis/oxidation (RPO) analysis ~~is an emerging~~has emerged as a powerful analytical technique ~~to deconvolve~~for characterizing sedimentary organic carbon (OC) ~~composition~~, bridging the knowledge gap between bulk carbon and molecular-level analyses~~. Generally, prior to RPO analysis~~. While acid~~ification~~ pretreatment is routinely employed ~~serves as an important pretreatment procedure~~ to remove carbonates prior to RPO analysis, ~~. Despite numerous studies evaluating the~~its methodological impacts remain poorly constrained ~~of acidification on~~compared to other geochemical ~~analyses~~measurements (e.g., δ^{13}C~~bulk carbon analysis~~)~~., the similar effect has been poorly recognized in RPO analysis. cid rinsing and acid fumigation are two typical and well-established acidification methods eliminating inorganic carbon. However, detailed protocols therein are most likely adopted based on conventional laboratory practices, assuming that the measurement precision is unaffected by experiment conditions. In fact~~In specific, OC and mineral dissolution caused by acidification lead to considerable loss of acid soluble OC and likely modification of the natural organo mineral interactions, which may significantly alter the RPO results.~~ Given the widespread utilization of RPO analysis in recent studies, a ~~careful~~comparative examination of pretreatment~~-induced~~ conditions is timely to ensure ~~biases is timely for ensuring more accurate and consistent results~~unbiased acquisition of thermochemical results.~~acidification can cause mineral dissolution and leaching of organic components, and therefore impacts the quantity and composition of residual POC considerably. Nonetheless, the effect of acidification on POC properties and the underlying mechanisms are ambiguous when relying solely on bulk measurements. In~~ T~~t~~his study ~~, we investigated~~systematically evaluates how decarbonation protocols influence ~~the pretreatment-induced impacts on~~ RPO results through comparative ~~by conducting replicate~~ analyses ~~on samples with~~of different ~~acidification~~pretreatment ~~procedures~~approaches. ~~POC properties following acidification using ramped temperature pyrolysis/oxidation (RPO) technique, in combination with bulk carbon analyses, to assess the impact of different decarbonation pretreatments on the sedimentary organic carbon (OC) measurements. Our results reveal~~We demonstrate that both acidification method (rinsing ~~or~~ *vs.* fumigation) and HCl concentration~~s~~ ~~under in acid rinsing are main factors~~significantly affect ~~altering~~ RPO ~~result of a sample~~thermograms, with ~~. dictating OC properties measured. Notably, despite negligible differences in bulk measurements, Notably,~~ ~~RPO results show distinct variations between these two acidification methods. In combination with other evidence,~~

our study suggests that, suggestive ofobserved differences attributed to the alteration of organic-inorganic associations, and selective leaching of acid-soluble OC. Notably, results from diluted acid rinsing are more similar exhibiting more similarity to the pristine conditions of the raw material. Based on comprehensive testing, we recommend diluted HCl rinsing with moderate reaction times (~ 12h) as the optimal pretreatment for most samples, while acknowledging that specific sample characteristics (e.g., organic lean, protein rich) may necessitate adjustments to the protocol require protocol adjustments. These finding highlight the importance of pretreatment protocolsconditions considerations in thermochemical decomposition studies. which is ubiquitous during acidification, drives the behaviour of POC properties that measured. Furthermore, we demonstrate that the characteristics of residual POC in RPO results of acid-rinsed samples are more proximalsimilar to pristine, natural states of the raw (natural) materials, whereas the strikingly discrepant differences between two acidification methods can be attributed mainly to the perturbation caused by calcium chlorides after acid fumigation.

1 Introduction

Organic geochemical proxies serve as powerful tools for reconstructing natural processes across modern and ancient environments. Current approaches primarily utilize either bulk analyses (e.g., organic carbon contents, $\delta^{13}C_{org}$) that provide integrated sample information, or molecular biomarkers (e.g., fatty acids, sterols) that offer source-specific insights. Bridging these scales, the ramped-temperature pyrolysis/oxidation (RPO) technique has emerged as a transformative approach that interprets organic carbon (OC) as a thermal reactivity continuum, effectively deconvoluting bulk signatures into component fractions (Cui et al., 2022; Hemingway et al., 2017a; Rosenheim et al., 2008). The RPO analysis progressively converts OC to CO_2 across a temperature gradient, with thermochemically labile OC being decomposed at lower temperatures and refractory OC at higher temperatures. Thus, OC of different sources (e.g., biogenic OC, rock-derived OC) and thermochemical behaviors can be, in part, discriminated in RPO analyses. This offers a window to "unfold" bulk C data to two-dimensional configurations characterized by OC species with relative quantities. This capability has significantly advanced studies of sediment chronology (Rosenheim et al., 2008, 2013; Venturelli et al., 2020), regional OC dynamics (Bao et al., 2018; Hemingway et al., 2018; Maier et al., 2025; Zhang et al., 2017; Zhang et al., 2022), and global organo-mineral interactions (Cui et al., 2022; Hemingway et al., 2019). Geochemical proxies are extensively utilized to expand our understanding of natural processes in modern environments and over geological time scales. Total organic carbon (TOC) content and stable carbon isotope ($\delta^{13}C$) of TOC, two simple and essential proxies therein, are critical in quantitative estimates. Numerous studies leveraged TOC and several environmental variables (e.g., denudation rates, sedimentation rates and water discharge) to constrain regional and global carbon fluxes (Dellinger et al., 2023; Smith et al., 2015; Hage et al., 2022; Zondervan et al., 2023); whereas $\delta^{13}C$ signatures are critical in discriminating sources of organic carbon (OC) (e.g., terrestrial or marine) or unraveling biological synthetic pathways (Berg et al., 2010; Meyers and Ishiwatari, 1993). Therefore, accurate measurements of above proxies are the premise of data interpretations. Current instrument advancing allows us to acquire relatively accurate data, with precisions of < 0.1% for TOC and < 0.1‰ for $\delta^{13}C$. However, artificially-induced methodological biases, while being frequently ignored, introduce

~~considerable and potentially more significant variations to the results. This is largely due to conventional adoption of different laboratory-based sample pretreatment methods.~~

Generally, ~~T~~the removal of inorganic carbon through ~~Prior to TOC and $\delta^{13}C$ measurements, the inorganic carbon is removed using acidification. Acidification~~decarbonation ~~is generally adopted to remove inorganic carbon~~represents a critical pretreatment step ~~before~~for ~~geochemical~~RPO analysis of~~on~~ sedimentary ~~organic carbon (~~OC~~)~~. ~~However, existing studies using bulk measurements, as a similar reference, have reported inconsistent, and sometimes contradictory, results regarding pretreatment effects (Brodie et al., 2011; Schlacher and Connolly, 2014), offering limited guidance for RPO-specific protocols. Typical~~ Currently, decarbonation approaches include~~employ~~ two different methods. Acid rinsing involves~~ include~~ direct addition of hydrochloric acid (HCl) solution to particulates in the aqueous phase followed by subsequent rinses with Milli-Q water~~ (i.e., acid rinsing) and~~ , ~~whereas~~while ~~acidification~~ acid fumigation ~~by~~ features direct exposure of particulates to HCl acid in the vaporous phase~~ (i.e., acid fumigation)~~ (Harris et al., 2001). Moreover, acid rinsing may vary in concentrations of HCl being applied (Kim et al., 2016; Pasquier et al., 2018), while ~~;~~. ~~whereas a~~Aacid fumigation in some cases is followed by water rinsing to remove chlorides~~ in recent studies~~ (Hemingway et al., 2017a). These various acidification pretreatments can yield diverse impacts on OC compositions (Brodie et al., 2011; Komada et al., 2008; Lohse et al., 2000; Schlacher and Connolly, 2014). Specifically, acid rinsing ~~might~~ can potentially ~~lead to~~ result in OC dissolution/hydrolysis (Fujisaki et al., 2022; Galy et al., 2007; ~~Schmidt and Gleixner, 2005~~Serrano et al., 2023), whereas acid fumigation is ~~speculated~~ thought to alter organo-mineral interactions (Plante et al., 2013) and is unsuitable for samples rich in carbonates (Hedges and Stern, 1984)~~–~~. ~~Additionally~~Furthermore, the choice between freeze-drying ~~versus~~ and oven drying~~ and the temperatures selected for the latter may result in~~introduces ~~further~~ additional~~ly~~ ~~uncertainties~~ variability in OC composition (De Lecea et al., 2011; Kim et al., 2016; McClymont et al., 2007). Despite widespread examination deployed for bulk parameters, systematic evaluation of pretreatment-induced artifacts remains notably lacking for RPO analysis (Bao et al., 2019; Hemingway et al., 2019). This knowledge gap necessitates comprehensive investigation of decarbonation pretreatments given the increasing adoption of RPO technique in organic geochemistry studies.

~~For decades~~~~As mentioned before~~~~, several studies compared the effect of acidification on OC analysis; however, the nuanced results remain inconsistent or even contradictory~~ relying on total organic carbon (TOC) and stable carbon isotope of OC ($\delta^{13}C_{org}$)~~ (Brodie et al., 2011; Schlacher and Connolly, 2014). The contentious results are somewhat conceivable~~understandable~~~~, since natural samples are a mixture of compounds and bulk OC data~~ (i.e., TOC and $\delta^{13}C_{org}$)~~ is the superposition~~addition~~ of myriad~~several~~ signals. In comparison with bulk measurements, the recently developed ramped-temperature pyrolysis/oxidation (RPO) technique has the advantage to interpret total OC as a reactive continuum and thus separate different signals~~ (Cui et al., 2022; Hemingway et al., 2017a; Rosenheim et al., 2008). The RPO analysis progressively converts organic carbon to CO_2 throughout a continuous heating process (Cui et al., 2022; Hemingway et al., 2017a; Rosenheim et al., 2008). Thermochemically labile OC is prone to decompose at early heating stage, whereas refractory OC converts to CO_2 at higher temperatures. Thus, OC of different sources (e.g., biogenic OC, rock-derived OC) within samples can be, in part, discriminated

~~in RPO analyses. This offers a window to "unfold" bulk C data to two-dimensional configurations characterized by OC species with relative quantities.~~ ~~The RPO analysis has been successfully applied in relevant studies on improved dating of sedimentary cores (Rosenheim et al., 2008, 2013; Venturelli et al., 2020), regional OC dynamics (Bao et al., 2018; Hemingway et al., 2018; Maier et al., 2025; Zhang et al., 2017; Zhang et al., 2022), and quantitative estimates on global sedimentary organo-mineral interactions (Cui et al., 2022; Hemingway et al., 2019). Nonetheless, as the majority of studies conduct acidification prior to RPO analysis, the diverse pretreatment conditions can likely lead to artificial biases. To current knowledge, the underlying impact of acidification on RPO results is understudied (Bao et al., 2019).~~

In this study, we systematically evaluate how pretreatment conditions influence RPO results by testing a suite of variables. ~~conducted a suite of contrasting experiments with various, aforementioned pretreatment conditions, including~~Variables of consideration include ~~different~~ acidification methods (rinsing *vs*. fumigation), concentrations of hydrochloric acid (1 N, 2 N, 4 N, 6 N and 12 N for fumigation), reaction durations (6 h, 12 h and 24 h), drying methods (freeze-drying *vs*. oven drying), ~~the temperature for~~ oven drying temperatures (45 °C *vs*. 60 °C), and ~~the temperature for~~acid reaction temperatures (ambient *vs*. 60 °C). Using RPO analyses supplemented with bulk measurements (TOC and $\delta^{13}C_{org}$), we assess the potential alteration of chemical structures and changes in OC quantities and compositions induced by pretreatment conditions. Our results establish ~~Following pretreatment, A~~a~~ll samples were subject to bulk (TOC and $\delta^{13}C_{org}$) and RPO measurements, of which the latter is used to decipher the methodological impacts on OC quantities and compositions. Apart from traditional criteria (e.g., the effectiveness of IC removal), we assessed the potential modification of chemical structures within samples induced by acidification pretreatments as another line of criterion in assessing the applicability of an acidification method. Finally, we summarize the likely influence of different pretreatment conditions on RPO analysis and further offer~~ the~~optimal~~ protocol~~s~~ that minimizes artifacts while maintaining analytical integrity, providing standardized pretreatment operations for this rapidly advancing~~expanding~~ techniques~~suggestions for acidification~~.

2 Materials and methods

2.1 Samples and preparation

Four samples with different properties were selected, including two lithified ancient sediments and two modern sediments. These samples were collected, respectively, from: (i) the Eocene Green River Formation (sedimentary rock, termed "~~1207-GR-11~~SR1"); (ii) the Permian-Triassic Meishan section (sedimentary rock, termed "~~MS05-135~~SR2"); (iii) the Yangtze River Estuary (modern sediment, termed "~~CJK-A6-3~~Sed1"); and (iv) Isfjorden fjord of Svalbard (modern sediment, termed "~~AREX R7~~Sed2"). Two rock samples (i.e., ~~1207-GR-11~~SR1 and ~~MS05-135~~SR2) have similar TOC values but contrasting carbonate contents, whereas the other two surface sediment samples (i.e., ~~CJK-A6-3~~Sed1 and ~~AREX R7~~Sed2) are similar in carbonate

contents~~are differentiated by TOC values~~, but are differentiated by TOC values ~~are similar in carbonate contents~~. All these samples were grounded into powder, homogenized, and divided into 13 aliquots, respectively, for subsequent processing.

2.2 Experimental design and operations

We conducted two ~~approaches of~~ contrasting acidification pretreatments, ~~i.e.~~i.e., acid rinsing ~~(EC-1 to EC-10)~~ and acid fumigation ~~(EC-11 and EC-12)~~. Particularly, ~~samples of~~ acid rinsing ~~were~~ was ~~pretreated~~ conducted with additionally various conditions to compare the influence of HCl concentrations ~~(EC-1, EC-2, EC-3 and EC-4)~~, acidification durations ~~(EC-1, EC-5 and EC-6)~~, drying methods and temperatures ~~(EC-1, EC-7 and EC-8)~~, the potential influence of heating at decarbonation reactions ~~(EC-1 and EC-9)~~ and prolonged exposure to concentrated acid ~~(EC-10)~~. ~~Additionally~~Furthermore, two ~~different~~sets of acid fumigation pretreatments~~methods~~ ~~(EC-11 and EC-12)~~ were carried out to compare with acid rinsing and to examine the ~~effect~~ impact of water rinsing following acid fumigation (Bao et al., 2019; Harris et al., 2001; Hemingway et al., 2017a). Major variables and corresponding parameters ~~For clarity purpose, we particularly termed EC-11 and EC-12 as "fume I" and "fume II", respectively.~~~~According to our preliminary results, the acidification method (rinsing *vs.* fumigation) and the HCl concentration applied in acid rinsing are thought to have major effects on RPO result. The details of these methods~~ are summarized in Table 1, while~~whereas. In addition,~~ detailed conditions and results of other minor factors (e.g., reaction time and drying method) are provided in the supplementary ~~material~~file ~~for completeness~~.

~~Each set of 12 aliquots were first acidified, where 10 were treated with acid rinsing method and two with acid fumigation (Table 1).~~ For acid rinsing, each aliquot (> 200 mg) was weighed in a 50 mL glass centrifuge tube, followed by the addition of HCl with a specific concentration (i.e., 1 N, 2 N, 4 N or 6 N). To ensure the complete removal of ~~that~~ IC ~~was completely removed~~, we gradually added HCl in excess. Moreover, we stirred solid-liquid mixtures during and after acidification using a portable vortex mixer. To investigate the effect of heating, one aliquot was maintained at 60 °C (± 3 °C) for 1 h after acidification. All ~~centrifuge tubes~~reactions were set~~left~~ for 6 h, 12 h, or 24 h according to designated experimental conditions (see Table S1). Afterwards, the supernatants were removed using pipettes after centrifugation and the residual solids were rinsed with Milli-Q water ~~for~~ three to four times to be neutralized.

For acid fumigation ~~method~~ ~~(EC-11, EC-12)~~, ~~eight~~ two sets of subsamples were weighed and placed in a glass petri dish (Φ 60 mm × 35 mm). Before fumigation, we carefully ~~instilled~~added several drops of Milli-Q water ~~into each subsample~~ to ~~form a thin film of water on the surface~~moisten subsamples (Harris et al., 2001; Yamamuro and Kayanne, 1995). Eight subsamples were then placed into a bilayer glass desiccator, being exposed to ~~together with~~ a glass beaker of ~ 50 mL 12 N HCl beneath ~~at the bottom. All subsamples were then exposed to acid vapors~~ at room temperature for 12 h. After fumigation, subsamples were supplied with two additional drops of aqueous HCl to verify the ~~effectiveness~~ completeness of decarbonation. This is based on the former practice that acid fumigation is not suitable for samples containing a great portion of $CaCO_3$ (Hedges and Stern, 1984). As expected, two subsamples of ~~1207-GR-11~~SR1 containing ~ 70% w/w $CaCO_3$ bubbled violently, indicating residual carbonate, whereas the others show no visible reaction. We then added HCl in excess to completely remove unreacted

$CaCO_3$ in ~~1207-GR-11~~SR1 subsamples. Afterwards, ~~four~~ one set of ~~EC-11~~ subsamples (SR1, SR2, Sed1, Sed2) therein were additionally rinsed with Milli-Q water for three times prior to freeze-drying.

Air drying at room temperature, oven drying and freeze-drying are typical drying methods, with the latter two being compared in this study. The majority of subsamples were freeze-dried at -60 °C for more than 24 h while ~~other subsamples~~two sets were dried in an oven at 45 °C or 60 °C for ~ 40 h (Table S1), respectively. Two different temperatures were adopted to examine possible influence of oven drying temperatures. Fumigated subsamples were dried at 60 °C ~~due to the concern that 45 °C was likely impotent to remove acid vapors completely, and thus corrode instruments.~~given that low~~er~~ temperature is inefficient into removing~~e~~ water vapor since the fumigated subsamples is prone to ~~absorbing~~~~moister~~moisture absorption~~water~~. To minimize the corrosive effect of vaporized HCl, fumigation subsamples ~~(those dried by oven)~~ were oven dried aside with sodium hydroxide flakes. After drying, subsamples were homogenized with an agate mortar and pestle. All glass containers were pre-combusted at 550 °C for 6 h to eliminate contaminants.

Table 1. Combinations of main experimental conditions investigated in this study, including acidification methods, HCl concentrations, reaction durations and temperature, as well as drying methods and temperature.

Acidification method[§]	HCl concentration	Reaction temperature	Duration	Drying method
Rinsing[§]	1 N	Ambient	12 h	Freeze-drying
Rinsing	2 N	Ambient	12 h	Freeze-drying
Rinsing	4 N	Ambient	12 h	Freeze-drying
Rinsing	6 N	Ambient	12 h	Freeze-drying
Fumigation + Rinsing	12 N	Ambient	12 h	Freeze-drying
Fumigation	12 N	Ambient	12 h	Oven drying, 60°C

~~[*]"EC" is the abbreviation of "experimental condition", and the suffixal numbers are for sorting purpose.~~[§]The ~~first line is the~~ control group is~~(~~ 1 N HCl~~)~~. We emphasize it is not necessarily to be the best choice of experimental condition. It is based on the experiment design and is only used to facilitate comparisons between different conditions.

~~[#]60°C water bath for the first hour, and then retained at room temperature.~~

2.3 Bulk carbon measurement

Each homogenized carbonate-free subsample was divided into two aliquots for bulk and RPO analyses (see Sect. 2.4), respectively. For the bulk carbon measurement, an aliquot containing ~ 200 µg OC was weighed, placed and wrapped in a tin capsule. Sample-containing tin capsules were transferred into the autosampler of a Thermo Fisher Scientific Flash IRMS elemental analyzer (EA) coupled to an Electron DELTA V Advantage isotope ratio mass spectrometer (IRMS). The resulting TOC and $\delta^{13}C_{org}$ values (Table 2) were then calibrated using three standards (i.e., USGS 40, USGS 62, USGS~~,~~ 64). The standard deviations (SDs) of TOC and $\delta^{13}C_{org}$ are~~were~~ 0.7% (relative) and 0.06‰ (absolute), respectively, based on USGS 40 (n = 5).

Table 2. Bulk and RPO parameters of all subsamples. Bulk parameters include TOC and $\delta^{13}C$; RPO parameters include the average activation energy (μ_E), the standard deviation of activation energy (σ_E), the fractions of OC with activation energy lower than 150 kJ mol^{-1} ($f_{E<150}$) and lying within 150–185 kJ mol^{-1} ($f_{150\leq E<185}$). Carbonate contents are included as well. Each row stands for a subsample subjected to a specific experimental condition. N. A. indicates not applicable.

Sample ID	Pretreatment	(%)	Bulk		RPO			
			TOC (%)	$\delta^{13}C$ (VPDB, ‰)	μ_E (kJ mol^{-1})	σ_E (kJ mol^{-1})	$f_{E<150}$	$f_{150\leq E<185}$
	EC-1	68.4	0.525	-28.95	188.51	22.97	0.046	0.309
	EC-2	69.5	0.519	-29.26	188.89	23.50	0.047	0.306
	EC-3	70.3	0.519	-28.90	188.91	24.16	0.051	0.307
	EC-4	70.5	0.520	-29.27	189.13	24.94	0.059	0.304
	EC-5	68.7	0.525	-28.95	191.46	23.30	0.040	0.270
	EC-6	68.5	0.522	-29.04	188.01	22.66	0.047	0.311
	EC-7	68.3	0.532	-28.94	189.40	22.88	0.045	0.296
	EC-8	69.1	0.521	-29.01	189.73	22.72	0.044	0.291
	EC-9	68.4	0.535	-28.96	187.83	22.95	0.048	0.316
	EC-10	70.2	0.533	-29.03	186.58	24.26	0.064	0.324
	EC-11	71.6	0.482	-29.03	188.08	24.54	0.058	0.313
	EC-12	N. A.	0.518	-28.94	165.85	19.41	0.174	0.705
	EC-1	8.8	0.586	-24.48	204.40	21.33	0.016	0.135
	EC-2	10.0	0.610	-24.46	203.94	21.27	0.015	0.138
	EC-3	11.0	0.597	-24.27	202.81	22.03	0.019	0.127
	EC-4	11.5	0.604	-24.15	197.39	23.47	0.025	0.243
	EC-5	7.7	0.584	-24.22	203.73	21.64	0.018	0.132
	EC-6	10.0	0.607	-24.43	205.10	22.19	0.019	0.129
	EC-7	8.4	0.580	-24.41	205.48	22.28	0.019	0.128
	EC-8	8.9	0.596	-24.49	202.89	21.71	0.020	0.141
	EC-9	10.7	0.596	-24.37	204.54	22.39	0.019	0.125
	EC-10	11.6	0.604	-24.57	194.20	25.11	0.034	0.297
	EC-11	12.8	0.587	-24.65	193.54	23.57	0.034	0.284
	EC-12	N. A.	0.568	-24.51	180.33	24.71	0.059	0.581
	EC-1	13.7	0.395	-22.82	175.58	35.14	0.205	0.447
	EC-2	14.5	0.388	-23.09	175.47	35.25	0.205	0.443
	EC-3	16.4	0.387	-22.90	176.48	35.33	0.192	0.438

~~EC-4~~	~~17.7~~	~~0.373~~	~~-23.08~~	~~177.18~~	~~35.55~~	~~0.186~~	~~0.443~~
~~EC-5~~	~~13.4~~	~~0.408~~	~~-23.09~~	~~175.54~~	~~35.28~~	~~0.206~~	~~0.444~~
~~EC-6~~	~~14.5~~	~~0.394~~	~~-22.77~~	~~177.36~~	~~35.23~~	~~0.194~~	~~0.430~~
~~EC-7~~	~~13.2~~	~~0.398~~	~~-22.66~~	~~175.35~~	~~35.71~~	~~0.220~~	~~0.435~~
~~EC-8~~	~~13.4~~	~~0.408~~	~~-22.80~~	~~174.56~~	~~35.58~~	~~0.230~~	~~0.432~~
~~EC-9~~	~~15.3~~	~~0.397~~	~~-22.88~~	~~177.39~~	~~35.15~~	~~0.189~~	~~0.432~~
~~EC-10~~	~~18.3~~	~~0.385~~	~~-23.30~~	~~178.32~~	~~35.22~~	~~0.173~~	~~0.445~~
~~EC-11~~	~~16.8~~	~~0.402~~	~~-22.99~~	~~175.82~~	~~34.95~~	~~0.198~~	~~0.444~~
~~EC-12~~	~~N. A.~~	~~0.440~~	~~-23.31~~	~~169.29~~	~~32.61~~	~~0.293~~	~~0.388~~
~~EC-1~~	~~13.8~~	~~1.224~~	~~-26.84~~	~~188.64~~	~~26.88~~	~~0.088~~	~~0.269~~
~~EC-2~~	~~15.0~~	~~1.153~~	~~-26.85~~	~~188.38~~	~~26.25~~	~~0.083~~	~~0.267~~
~~EC-3~~	~~17.2~~	~~1.131~~	~~-27.16~~	~~187.51~~	~~25.61~~	~~0.069~~	~~0.323~~
~~EC-4~~	~~18.3~~	~~1.144~~	~~-27.03~~	~~182.93~~	~~26.08~~	~~0.083~~	~~0.425~~
~~EC-5~~	~~13.2~~	~~1.210~~	~~-26.89~~	~~189.99~~	~~26.59~~	~~0.085~~	~~0.244~~
~~EC-6~~	~~14.6~~	~~1.147~~	~~-26.80~~	~~190.39~~	~~26.33~~	~~0.079~~	~~0.240~~
~~EC-7~~	~~13.2~~	~~1.175~~	~~-27.12~~	~~187.66~~	~~26.94~~	~~0.095~~	~~0.289~~
~~EC-8~~	~~13.6~~	~~1.152~~	~~-26.92~~	~~187.60~~	~~27.02~~	~~0.096~~	~~0.291~~
~~EC-9~~	~~15.5~~	~~1.179~~	~~-27.20~~	~~189.16~~	~~26.12~~	~~0.075~~	~~0.263~~
~~EC-10~~	~~17.7~~	~~1.182~~	~~-26.84~~	~~183.56~~	~~26.23~~	~~0.082~~	~~0.418~~
~~EC-11~~	~~20.9~~	~~1.128~~	~~-27.13~~	~~180.57~~	~~25.71~~	~~0.097~~	~~0.461~~
~~EC-12~~	~~N. A.~~	~~1.230~~	~~-26.87~~	~~183.41~~	~~30.45~~	~~0.111~~	~~0.449~~

2.4 ~~RPO~~ Ramped-temperature pyrolysis/oxidation analysis

The integrated ~~RPO~~ ramped-temperature pyrolysis/oxidation (RPO) system utilized here comprises ~~is~~ primarily ~~comprised~~ of a carrier gas unit, a programmable pyrolysis furnace and an infrared CO_2 analyzer (Supplementary file Fig. S1). The pyrolysis furnace consists of two insulated furnaces (i.e., the upper and the lower) with thermocouples mounted ~~equipped~~. A large quartz tube was inserted into the middle chamber of furnaces with catalytic wires (Cu, Pt, Ni) ~~mounted~~ placed in the lower half. During each RPO run, a smaller-sized quartz reactor was packed with an aliquot of sediment containing ~1 mg OC near~~at~~ the~~its~~ bottom end, which was~~is~~~~was~~ then introduced into the upper half of the large quartz tube. Afterwards, the upper furnace was heated at a constant ramping rate of 5 °C min^{-1} from ~ 60 °C to > 1000 °C with steady carrier gas flow rates, whereas the lower furnace was maintained isothermally at 800 °C. The carrier gas flow in the inner quartz tube ~~was~~ consists of 27 mL min^{-1} ~~of~~ helium ~~mixed with~~and 3 mL min^{-1} diluted oxygen (5% oxygen). This sub-oxidation mode was consistently adopted in this study to circumvent possible charring during ~~heating~~pyrolysis as illustrated by previous studies (Huang et al., 2023; Stoner et al., 2023; Williams et al., 2014). Further, an additional 5 mL min^{-1} pure oxygen was introduced to the interface of two furnaces

to completely oxidize vaporized OC fragments downstream. For blank control, quartz tubes were combusted at 1000 °C for ~ 8h prior to RPO analyses. Generally, the precision of the ramping temperature rate was < 0.2%; ~~whereas~~ evolved CO_2 concentrations were calibrated against standard gas containing 2000 ppm CO_2.

~~We also noted that~~~~Notably, the residual chloride in sediments may generate chlorine gas under ramping temperatures, which. The chlorine gas further reacts with catalytic wires, and thus, distorts the authenticity of thermograms (Hemingway et al., 2017b; Huang et al., 2023). This consideration was of no concern to acid rinsing aliquots as the majority of chloride ions were removed after repeated rinses and dilution, whereas considerable amount of chloride in acid fumigation counterparts, especially those dried by oven, surged the risk. To continuously track the status performance of catalytic wires, we ran an in-house sample (termed "Irati T2") as the standard, under the same conditions (ramped rate, carrier gas flow rate and O_2 concentration), before and after RPO analysis of those fumigation-treated, oven-dried aliquots. The RPO results of standard samples are presented in the supplementary file (Fig. S1).~~

2.5 Simulation experiment with addition of calcium chloride

Notably, the residual chloride in sediments may generate chlorine gas under ramping temperatures, which further reacts with catalytic wires, and thus, distorts the authenticity of thermograms (Hemingway et al., 2017b; Huang et al., 2023). This consideration was of no concern to acid rinsing aliquots as the majority of chloride ions were removed after repeated rinses and dilution, whereas considerable amount of chloride in acid fumigation counterparts, especially those dried by oven, surged the risk. To continuously track the performance of catalytic wires, we ran an in-house sample (termed "Irati T2") as the standard, under the same conditions (ramped rate, carrier gas flow rate and O_2 concentration), before and after RPO analysis of those fumigation-treated, oven-dried aliquots. The RPO results of standard samples are presented in the supplementary file (Fig. S2).

To further verify the impact of chlorine gas during RPO analysis, a $CaCl_2$ addition experiment was carried out with the in-house standard (Irati T2), by assuming that chlorine gas is generated at elevated temperatures from the decomposition of $CaCl_2$, the major chloric constitute in acid fumigated sediments. Specifically, one aliquot of Irati T2 was added with ~ 30 mg $CaCl_2$ powders, whereas another aliquot of Irati T2 was added with ~ 30 mg $CaCl_2$ powders, moistened with Milli-Q water, oven dried, and then rinsed three times to remove chloride ions (part of Ca^{2+} and other cations co-precipitated with OC). The amount of $CaCl_2$ added (~ 30 mg) was carefully determined as it represents the median of potential $CaCl_2$ precipitates in four acid fumigated subsamples (~ 20 mg to > 100 mg). Subsequently, two aliquots were successively analyzed for RPO and compared with results of raw Irati T2 material.

2.6~~5~~ Data analysis

~~Based on the initial experimental design, we determine EC 1 as the control groups to simplify our calculation of relative variations of bulk results. However, we clarify that the determination of a particular group as the control does not change or bias our calculation of variables and thus conclusions drawn. For convenience, we number the four samples from 1 to 4,~~

~~following the same order in Table 2, and sort subsamples by the order from 1 to 12 according to pretreatment procedures. Then, we can quantify the relative changes of bulk TOC in our sample set as~~

$$\Delta(TOC)_{i,j} = \frac{TOC_{i,j} - TOC_i^*}{TOC_i^*}, i = 1, \ldots, 4, j = 2, \ldots, 12, \quad (1)$$

~~where $TOC_{i,j}$ is the TOC value of the i-th sample treated by the j-th experimental condition (i.e., EC-j) and TOC_i^* is the TOC value of the i-th sample with control conditions (i.e., EC-1). Note that the results derived from Eq. (1) are relative changes, offsetting the discrepancies between samples with variable TOC values. Similarly, we can derive the changes of $\delta^{13}C$ signatures as~~

$$\Delta(\delta^{13}C)_{i,j} = \delta^{13}C_{i,j} - \delta^{13}C_i^*, i = 1, \ldots, 4, j = 2, \ldots, 12, \quad (2)$$

~~**noting that it is the absolute form, which is different from Eq. (1). The results derived from Eqs. (1) and (2) are either positive or negative, corresponding to enrichment or depletion, respectively, relative to the control groups.**~~

Based on aforementioned experimental design, RPO analyses ~~and the generation of thermograms~~ were conducted for all acidified aliquots and homogenized raw (unacidified) materials. RPO thermograms were further converted to probability density distributions (i.e, p[E]) by the inverse method (Hemingway et al., 2017a), following an open-source package "rampedpyrox" in Python (Hemingway, 2017). Three fundamental parameters, including the mean value of E (termed "μ_E"), the standard deviation of E (termed "σ_E"), and the proportion of OC within a specific~~the~~ range ~~-~~ of E ~~from *a* kJ mol^{-1} to *b* kJ mol^{-1}~~ (e.g., *a* kJ mol^{-1} to *b* kJ mol^{-1}; termed "$f_{a<E<b}$"), were calculated for statistic analyses. The default value of the lower bound "a" is 50 kJ mol^{-1}, if not specified.

The mean of E was calculated as:

$$\mu_E = \int_0^\infty Ep(E)dE \quad (\cancel{3}1)$$

The square root of the variance of E was calculated as:

$$\sigma_E = (\mu_{E^2} - [\mu_E]^2)^{1/2} \quad (\cancel{4}2)$$

The proportion of OC within a specific E range (a kJ mol^{-1} to b kJ mol^{-1}) was calculated as:

$$f_{a<E<b} = \int_a^b p(E)dE \quad (\cancel{5}3)$$

RPO parameters measured and/or calculated as well as bulk parameters of all subsamples are listed in Table S2. Based on RPO results of the in-house standard (Irati T2; n=8), the standard deviation (SD) of μ_E is 0.50 kJ mol^{-1}, and SD of σ_E is 0.18 kJ mol^{-1}, denoting excellent reproducibility.

~~2.6 Simulation experiment with addition of calcium chloride~~

~~The two acidification methods adopted in this study (i.e., acid rinsing and fumigation) can result in completely different content of calcium chloride in sediments after pretreatment. To simulate the impact of $CaCl_2$ generated during acid fumigation, a $CaCl_2$ addition experiment was carried out with the in-house standard (Irati T2). Under this experiment, one aliquot of Irati T2 was added with ~ 30 mg $CaCl_2$ powders, whereas another aliquot of Irati T2 was added with ~ 30 mg $CaCl_2$ powders, moistened with Milli-Q water, oven dried, and then rinsed three times to remove chloride ions (part of Ca^{2+} and other cations co-precipitated with OC). The amount of $CaCl_2$ added (~ 30 mg) was carefully determined as it represents the median of potential $CaCl_2$ precipitates in four acid fumigated subsamples (~ 20 mg to > 100 mg). Subsequently, two aliquots were successively analyzed for RPO and compared with results of raw Irati T2 material.~~

3 Results and discussion

~~3.1 A snapshot of the influence from each factor on bulk parameters~~

~~Compared with the control groups, most TOC and $\delta^{13}C$ results exhibit marginal fluctuations within a range of ± 5% and ± 0.4‰, respectively (Fig. 1). It should be noticed that none of the factors exert an unambiguous control on bulk results. To better grasp net effects of each factor, we arithmetically averaged deviations of four samples under each condition (Fig. 1). Enhanced loss of OC is observed under elevated concentrations of HCl (1 N to 6 N) (Fig. 1b). The consistent depletion of $\delta^{13}C$ signatures with 2 N to 6 N HCl in relative to control conditions (1 N) indicates preferential loss of ^{13}C-enriched moieties. It was recognized that hydrolysable OC (e.g., amino acids), in general, are enriched in ^{13}C relative to bulk average and the acid-insoluble counterpart (Hwang and Druffel, 2003; Wang et al., 1998). Thus, we speculate that lower bulk $\delta^{13}C$ signatures after acid rinsing are attributed to the preferential loss of hydrolysable OC. Such observation is further corroborated by stronger loss of OC and larger offsets of $\delta^{13}C$ values of EC-11 (fume I), which was fumigated with 12 N HCl and rinsed afterwards with Milli-Q water. It suggests that a greater proportion of sedimentary OC is possibly hydrolyzed under concentrated HCl and further washed away (Fig. 1b) (Bao et al., 2019; Brodie et al., 2011).~~

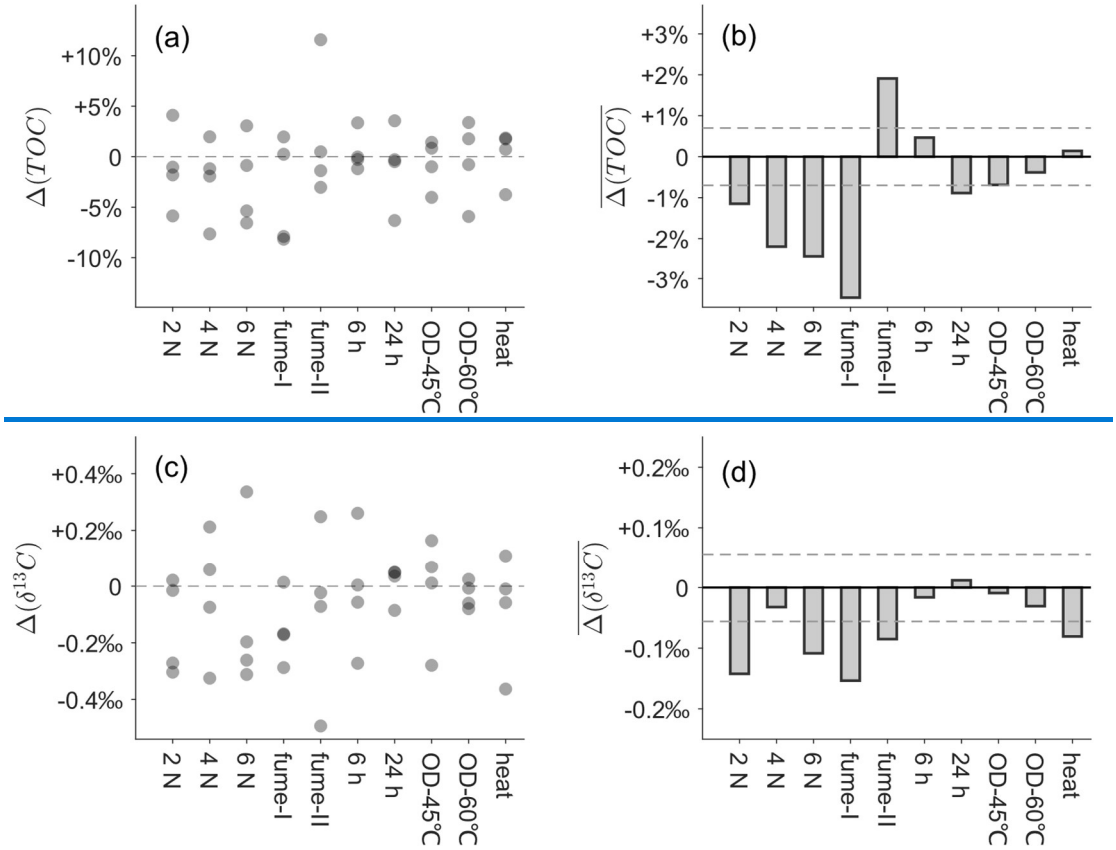

~~**Fig 1:** An integrated assessment of influence of all factors on bulk parameters. **(a)** and **(c)** exhibit deviations of each experiment from the control groups (EC 1) at the sample level. The control groups (EC 1) are not included, whereas each grey dot represents one subsample after a particular pretreatment. The datum lines (dash lines) in **(a)** and **(c)** are reference values of TOC and $\delta^{13}C$. Grey dots above and below the datum lines indicate relative enrichment or depletion, respectively. To delineate the net effects of all factors, bar plots of the average deviations (i.e., the mean value of four grey dots in vertical) are correspondingly plotted in **(b)** and **(d)**. The dash lines in **(b)** and **(d)** are standard deviations in measurements of TOC (±0.7%) and $\delta^{13}C$ (±0.056‰), respectively.~~

~~In contrast, EC 12 (fume II) without water rinsing exhibits higher TOC contents than samples with water rinsing, suggestive of efficient retention of labile components that are hydrolyzed and dissolvable. Surprisingly, the TOC contents of fume II offset the most with that of fume I and are even higher than those of samples under control conditions. It implies that the control condition as defined in this study may still lead to the loss of a proportion of labile, dissolvable OC, rendering former postulations (Huang et al., 2023). However, despite mitigated OC loss on average, some fume II subsamples exhibit slightly~~

~~lower TOC values than those under the control condition (Fig. 1a), presumably attributed to volatilization of labile materials during the oven drying process (Bisutti et al., 2004; Caughey et al., 1995).~~

~~Other experimental conditions, including the reaction time, drying method and reaction temperature, show inconspicuous changes in TOC and $\delta^{13}C$ values. In fact, most values are close to or within ranges of standard deviations (Fig. 1), indicative of their limited influence on bulk parameters. However, we noticed that prolonged reaction and oven drying process slightly promote OC loss, whereas heating makes no difference (Fig. 1).~~

~~Overall, acid fumigation versus acid rinsing and HCl concentrations for the latter are two key factors to consider for acidification conditions, whereas other factors exert minimal effects on bulk results. Conceivably, this is likely also the case for their influence on thermographic properties. In the next section, we continue to decipher the mechanisms of discrepant TOC and $\delta^{13}C$ values caused by these two key factors based on the thermochemical analysis.~~

3.~~2~~1 HCl concentration ~~biases~~influences on thermochemical properties and potential mechanisms

~~RPO~~ Ramped-temperature pyrolysis oxidation (RPO) results show that samples after acid ~~acidification, whether by fumigation or~~ rinsing~~,~~ exhibit pronounced deviations in thermograms and energy distributions~~, which are more prominent than results recorded by bulk parameters (TOC and $\delta^{13}C$)~~ (Table S2). ~~In terms of subsamples treated by acid rinsing, e~~Although variations of~~hanges in~~ secondary factors (e.g., reaction time, drying methods and temperatures) exert insignificant or erratic influences on the distribution patterns of thermograms (Supplementary file Fig. S3~~2~~ and S4~~3~~). ~~In contrast~~, ~~, almost all the~~ thermographic patterns exhibit~~show~~ ~~definitely~~ systematic ~~changes~~shifts~~gradation~~ along the gradient of HCl concentrations (Fig. ~~2~~1).

To ~~reconcile and depict~~~~explicitly~~ illustrate the inherent consistency between ~~coincident variations of~~ thermograms and HCl concentrations being applied, we orthogonally decomposed evolutionary trends of thermograms into two directions. Changes in the vertical orientation are interpreted as enrichment or loss of OC, whereas horizontal shifts represent alterations in thermal stability and, presumably, structural distortion (Fig. 1). Intriguingly, all four samples in this study exhibit distinct patterns encompassing different vertical and horizontal variations.

Notably, the intensity of OC decomposition at T_{max} (temperature of maximum CO_2 concentrations) diminishes progressively with increasing HCl concentrations for lithified rock samples (i.e., ~~1207-GR-11~~SR1 and ~~MS05-135~~SR2) (Fig. ~~2~~1a and ~~2~~1b), consistent with slightly broadening thermograms and elevations in standard deviations of activation energies (σ_E) (Table S2). Since T_{max} values are ~ 540 °C and ~ 600 °C for ~~1207-GR-11~~SR1 and ~~MS05-135~~SR2, respectively, within the decomposition temperature window of heavily altered petrogenic OC (Hemingway et al., 2018; Venturelli et al., 2020), such decreases in peak CO_2 decomposition also indicate a reduction in the content of thermochemically recalcitrant OC (Bao et al., 2019). ~~In terms of other two samples~~In contrary, whereas changes are in~~no~~ significant ~~changes are seen~~ in ~~the sediment CJK-A6-3~~Sed1 (Fig. ~~2~~1c)~~ along the HCl concentration gradient~~, a horizontal shift of thermograms towards lower temperatures has been observed for ~~the sediment AREX-R7~~Sed2 (Fig. ~~2~~1d), suggestive of OC being thermochemically more labile as a consequence

of elevated HCl concentrations. With the exception of ~~CJK-A6-3~~Sed1, the uniform alteration of OC toward labile thermochemical properties, by lowering proportions of recalcitrant OC and/or shifting thermograms to lower temperatures, implies systematic effects ~~caused~~ induced by HCl concentrations (Fig. ~~2~~1).

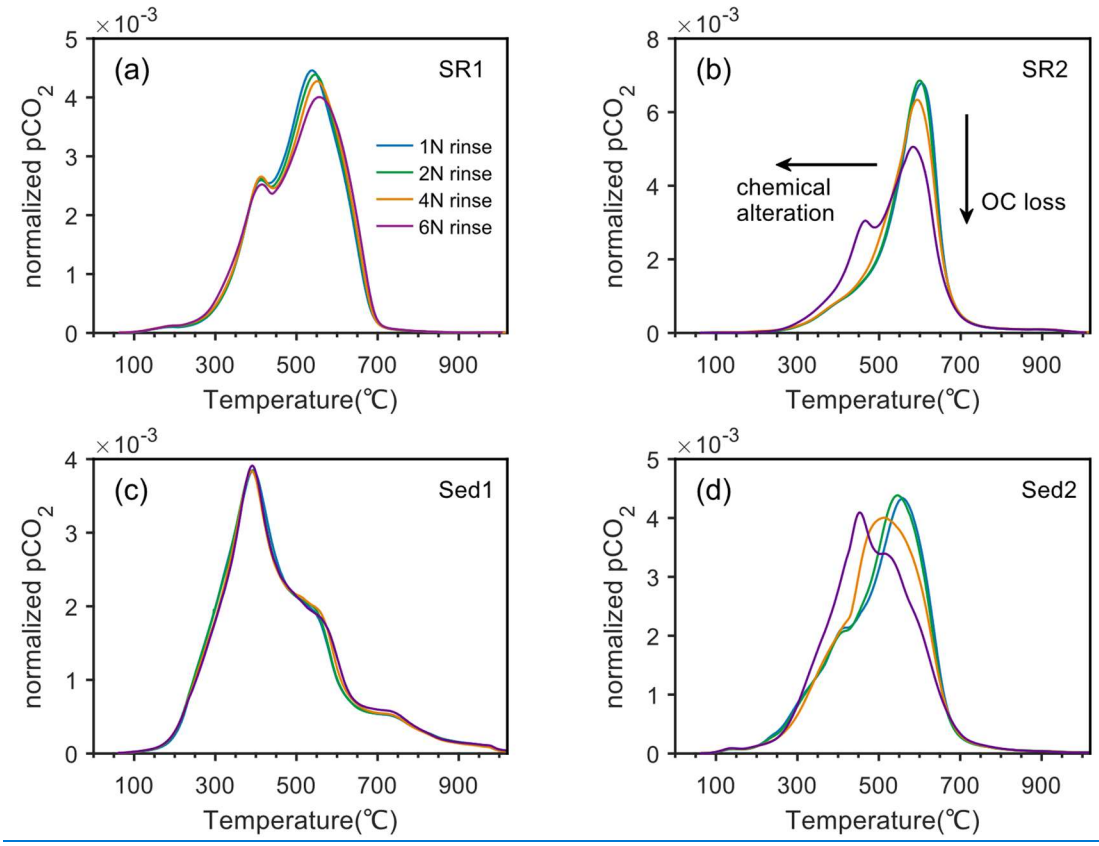

Fig ~~2~~1: Normalized thermograms of subsamples rinsed with different concentrations of HCl. **(a)**, **(b)**, **(c)** and **(d)** are subsamples of ~~1207-GR-11~~SR1, ~~MS05-135~~SR2, ~~CJK-A6-3~~Sed1 and ~~AREX-R7~~Sed2, respectively. ~~See methods for the definition of EC-1 to EC-4.~~Two orthogonal arrows in panel **(b)** indicate different variation modes of thermograms.

Pronounced variations in thermograms and accordingly enhanced lability of OC ~~rinsed with~~under concentrated HCl are likely attributed to structure alteration of mineral matrices and their interactions with OC, in addition to leaching of a fraction of dissolvable OC through acid rinsing. In general, OC exists in sediments in the form of free molecules, aggregates, bound to minerals, or as kerogens. A c~~C~~onsiderable amount of OC in sediments is stabilized as OC-Fe chelates (Lalonde et al., 2012; Mackey and Zirino, 1994), coated onto mineral surfaces (Mayer, 1994a, b; Vogel et al., 2014), trapped in carbonate matrices (Ingalls et al., 2004; Summons et al., 2013; Yang et al., 2025; Zeller et al., 2020, 2024) and preserved in mineral interlayers (Blattmann et al., 2019; Huang et al., 2023; Kennedy et al., 2002). The dissolution of carbonates under diluted HCl would release OC initially preserved in the carbonate matrix (Zeller et al., 2020), whereas other minerals and OC associated therein

are undisturbed. Through ~~the addition of HCl solution~~carbonate dissolution, a minimal proportion of OC is dissolved in the aqueous phase and washed away at the following water rinsing steps. In comparison, elevated concentrations of HCl would further attack other minerals (e.g., iron oxides, clay minerals) and leach metal ions into solution (Brodie et al., 2011; Fujisaki et al., 2022; Kumar et al., 1995). In fact, former studies demonstrate~~d~~ that concentrated acids cause metal isotopic fractionations by leaching minerals disproportionally (Fernandez and Borrok, 2009; Rongemaille et al., 2011). Such ~~postulation~~ observation is in consensus with elevated mass loss ~~with~~ under concentrated HCl in this study (Table S2). On one hand, concentrated HCl promotes the leaching of OC by releasing and dissolving molecules initially associated with minerals. On the other hand, the destruction of mineral matrix induces profound structural alterations of organic-inorganic complexes (Bao et al., 2019), and reduces organo-mineral binding energy, which is evidenced by shiftings ~~of some samples~~E distributions toward lower activation energies (Table S2). ~~Therefore, patterns of thermograms and energy distributions coeval with variations in TOC contents, isotopic values and mass loss along the gradient of HCl concentrations (Table 2).~~

Diverse thermographic shifts along HCl gradients ~~DiscrepantDifferent responses to HCl also~~ suggest sample-specific ~~that~~ impacts of ~~effects of~~ acidification conditions on RPO thermograms ~~are sample-specific~~ and thus warrant ~~a~~ careful examination of sample properties. We propose that ~~diverse~~~~different~~contrasting variations among samples ~~responses of samples~~ are primarily driven by organo-mineral interactions and diagenetic alterations. ~~Our T~~~~two lithified sediments,~~ A~~a~~lbeit with contrasting carbonate contents, two lithified sediments respond similarly to elevated HCl concentrations (i.e., denudation in main peak heights and broadening thermograms) without significant thermographic shifts. This is likely due to strong organo-mineral interactions established and homogenized OC properties with time (Craddock et al., 2018; Kennedy et al., 2014). As diagenesis proceeds, processes including the breakdown of biopolymers, modification of functional groups and secondary condensation reactions take place successively (Burdige, 2007), leading to enhanced degrees of reconstruction and lower overall vulnerability to external alterations.

In comparison, ~~AREX R7~~Sed2 is a modern high-latitude surface sediment with limited diagenetic alteration and hydrodynamic sorting. Accordingly, the majority of OC is likely bound to minerals loosely, and thus would respond considerably to acid concentrations through reversibly breaking or re-establishing weak bonds, which is expressed as horizontal shifts of thermograms (Fig. ~~2~~1). Conversely, ~~However, CJK A6-3~~Sed1 represents sediments deposited under ~~the~~ aerobic~~oxic~~ settings on an expansive shelf after extensive degradation along fluvial systems. Consequently, OC preserved therein, regardless of its terrestrial or marine origin, is strongly bond to minerals and thus exhibits sluggish responses to increasing HCl concentrations with nearly overlapping thermograms (Fig. ~~2~~1) (Huang et al., 2023).

3.~~3~~2 Thermographic distortion by acid fumigation and the effect of calcium chloride

Significant discrepancies ~~of RPO thermograms~~ are observed in RPO thermograms between acid fumigation and acid rinsing ~~results~~ (Fig. ~~3~~2), aswith ~~. To simplify potential variables and to compare differences between acid fumigation and rinsing, we combined and averaged thermograms of acid-rinsed subsamples. Direct comparison between acid fumigation and rinsing~~

~~suggests that~~ conventional acid fumigation (~~fume I~~i.e., without water rinsing) largely lowers or diversifies thermochemical stability of OC. This ~~, which~~ is ~~possibly~~ related to two putative mechanisms. On one hand, acid fumigation establishes an ambient environment of vaporized HCl, which further attacks sample particles through formation of concentrated HCl solution (Bao et al., 2019). On the other hand, $CaCl_2$ forms after decarbonation further interacts with OC and alters the structure of OC and organo-mineral interactions ~~accordingly~~ during combustion (Wu et al., 2024).

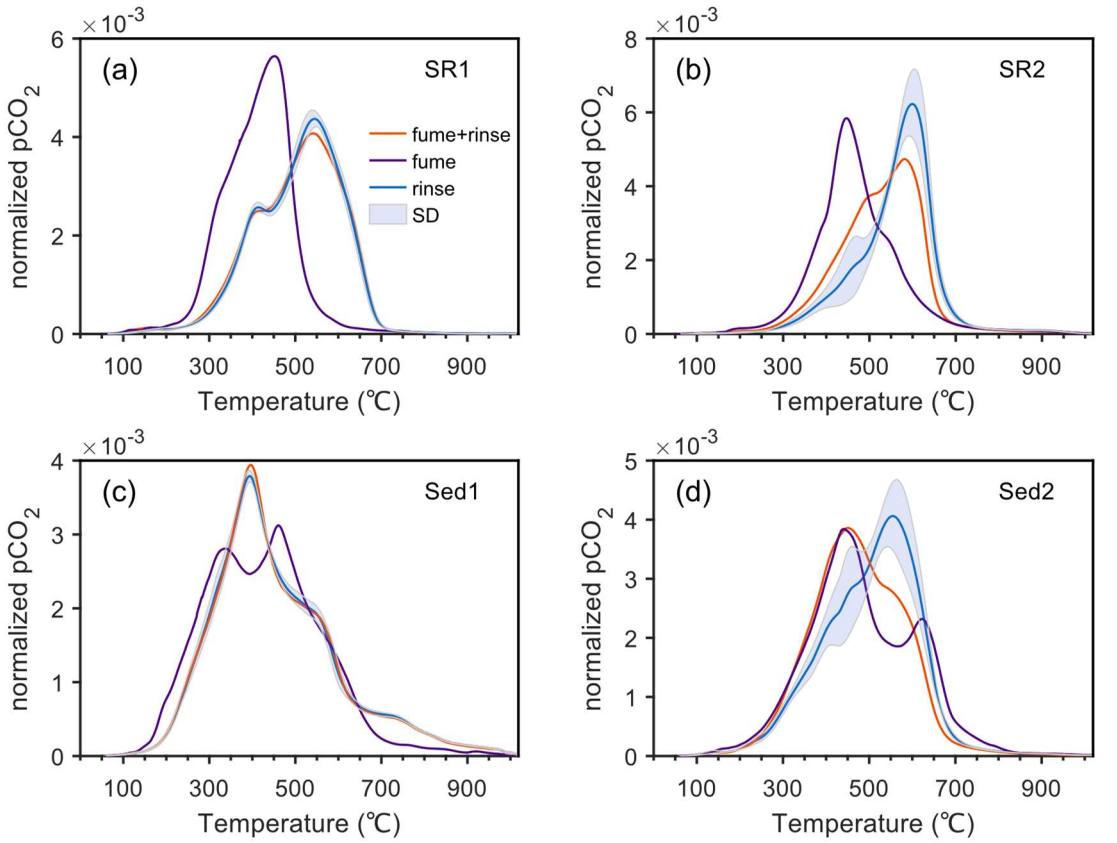

Fig ~~3~~2: Normalized thermograms of subsamples after acid rinsing and fumigation. **(a)**, **(b)**, **(c)** and **(d)** represent subsamples of ~~1207-GR-11~~SR1, ~~MS05-135~~SR2, ~~CJK-A6-3~~Sed1 and ~~AREX-R7~~Sed2, respectively. ~~Yellow~~Purple curves and ~~dark brown~~orange curves ~~stand for~~ present subsamples acidified ~~by EC-11 (or fume I) and EC-12 (or fume II)~~using typical fumigation method and fumigation-rinsing method, ~~whereas~~while blue curves are mean values of ~~EC-1 to EC-10~~ acid rinsed subsamples (Table S1) with shaded intervals representative of standard deviations.

~~To unravel potential mechanisms of contrasting RPO thermograms after acid fumigation, we first evaluate t~~The impact of concentrated HCl ~~concentration~~ generated from acid vapor condensation is assessed through~~. To do so, we add~~~~with an additional~~~~the group of~~ acid fumigation-rinsing ~~control~~ experiment (~~fume I~~fumigation + rinsing; Table 1). Under this

experiment, ~~, in which~~ acid fumigated powders are~~were~~ further rinsed with Milli-Q water to remove HCl and $CaCl_2$~~.~~, which eliminates potential effects of residual HCl and CaCl2 vapor upon RPO analysis. Results show that thermograms of ~~fume I~~ fumigation-rinsing subsamples are, in general, comparable to those of HCl rinsed subsamples, ~~but and~~ exhibiting a ~~constant gradation~~consistent thermographic shift toward more concentrated HCl conditions ~~pretreatments~~ (e.g., 12 N HCl) (Fig. 2). ~~following HCl concentrations (Fig. 32). Explicitly, thermographic patterns of fume I fumigation-rinsing subsamples are consistent with results anticipated for concentrated HCl pretreatments (e.g., 12 N HCl).~~ Therefore, it indicates that ~~the concentrated HCl solution~~acid fumigation through the ~~dissolution~~ condensation of HCl vapor exerts a noticeable and systematic impact on the thermochemical characteristics of sedimentary OC.

The contrasting ~~difference~~ results between ~~fume II~~ typical fumigation ~~method~~ and ~~other water-rinsing experiments, including fume I~~fumigation-rinsing methods ~~as well as HCl rinsing,~~ suggest~~s~~ that $CaCl_2$ may play an additionally dominant role in modifying thermochemical properties of sedimentary OC, given the residual $CaCl_2$ being the main difference between ~~fume II~~ these two groups~~fumigation method and others~~. We propose that $CaCl_2$ may influence thermograms in two ~~distinct~~ contrary ways. First, HCl or chlorine gas may boost the breakup of organo-mineral bonds or covalent OC bonds ~~in OC~~ and thus stimulate the decomposition of OC at elevated temperature (Plante et al., 2013). In the meantime, ~~it is noteworthy that in our system~~ chlorine gas generated through~~by~~ the decomposition of $CaCl_2$ under high temperatures ~~also~~ interacts directly with the catalytic wires (Hemingway et al., 2017b), corrodes reactor tubes (Supplementary file Fig. S54), and thus, influences the thermochemical reaction rates. ~~Furthermore~~Conversely, calcium ions (and other metal ions) may enhance organo-cation interactions or facilitate organo-mineral aggregations (Keil and Mayer, 2014; Rowley et al., 2018; Sowers et al., 2018), and thus complicate reaction kinetics. It has been demonstrated that Ca^{2+} in soils and sediments enhances the sorption and stabilization of OC (Feng et al., 2005; Rowley et al., 2018). However, the proposed Ca-stabilization mechanism contradicts the observation of fumigated OC being more labile ~~nature of fume II fumigated subsamples~~. Therefore, it is possible that HCl and chlorine gas, other than the calcium ion, play a more important role in affecting the ultimate thermochemical decomposition of sedimentary OC after fumigation.

~~To further demonstrate t~~The assumption of thermochemical biases induced by $CaCl_2$ ~~(fume II),~~ is further verified by ~~we carried out a~~the $CaCl_2$ addition experiment ~~(Sect. 2.6)~~ with the in-house standard (Irati T2). ~~Under this experiment, one aliquot of Irati T2 was added with ~ 30mg $CaCl_2$ powders, whereas another aliquot of Irati T2 was added with ~ 30mg $CaCl_2$ powders, moistened with Milli-Q water, oven dried, and then rinsed three times to remove chloride ions (part of Ca^{2+} and other cations co-precipitated with OC). The amount of $CaCl_2$ added (~ 30mg) was carefully determined as it represents the median of potential $CaCl_2$ precipitates in four fume II subsamples (~ 20mg to > 100 mg). Subsequently, two aliquots were successively analyzed for RPO and compared with results of raw Irati T2 material (Fig. 4).~~ Consistent with the assumption above, the thermogram~~s~~ of Irati T2 with the addition of $CaCl_2$ is distinct from those of raw ~~Irati T2~~material and $CaCl_2$ addition-rinsing ~~that with water rinsing after addition of $CaCl_2$ resemble each other and are distinct from that with the addition of $CaCl_2$, but without water rinsing~~ (Fig. 3). Therefore, it ~~further~~ demonstrates that thermographic distortion of ~~fume II~~ fumigated

subsamples is most likely an artifact ~~due to the presence~~ of $CaCl_2$. We further measured the raw Irati T2 material before and after the analyses of ~~fume H~~fumigated subsamples, which apparently corrodes and melts catalytic wires. ~~Constant~~ Invariable thermograms of Irati T2, ~~thermogramsyet~~ significantly declined CO_2 yield after~~post~~ the analysis of fumigated subsamples suggest ~~an~~ insignificant ~~influence of~~ thermographic distortions but~~, while~~ incomplete catalytic conversion of CO to CO_2 after the corrosion of the catalytic wires (Fig. S2). ~~suggest that the corrosion of catalytic wires may not exert an apparent influence on thermographic distortions (Supplementary file Fig. S21). However, it is noteworthy that the CO_2 yield after the corrosion of catalytic wires declines significantly, likely due to the incompletely catalytic conversion of CO to CO_2.~~ Overall, the above results suggest that $CaCl_2$ biases the thermographic distortion by dictating the pyrolytic breakdown of sedimentary OC.

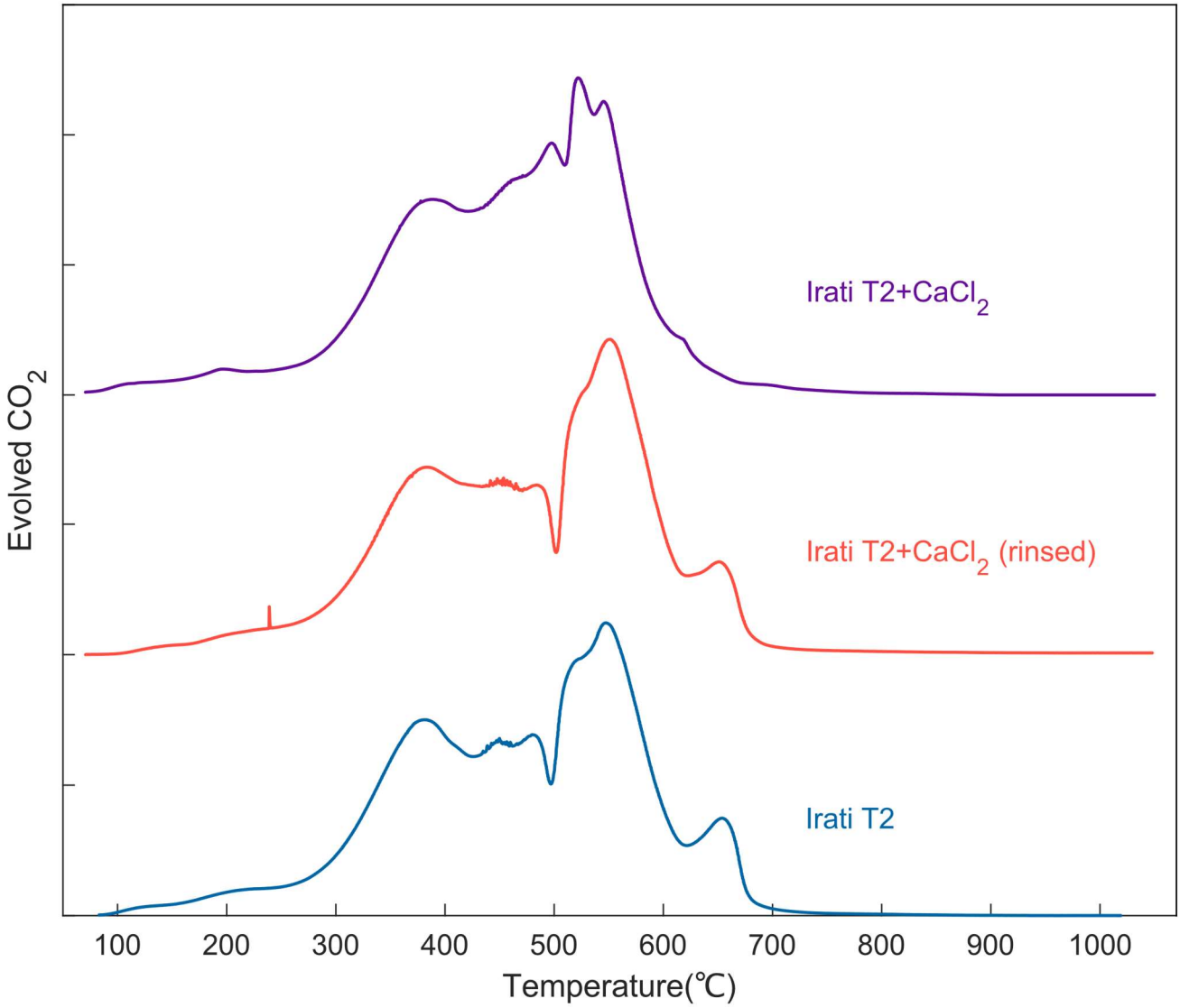

Fig 43: Parallel thermograms of the in-house standard (Irati T2) with distinct treatments. From bottom to top, the blue curve is Irati T2 without any extra treatment; the dark orange curve represents Irati T2 mixed with ~30 mg $CaCl_2$ and then rinsed with Milli-Q water preceding RPO analysis; ~~whereas~~ the dark ~~brown~~purple curve is Irati T2 with addition of ~30 mg $CaCl_2$ preceding RPO analysis. All samples were analyzed in sequence within two days to alleviate potential systematic biases with time.

3.43 Decarbonation pretreatments deviate thermochemical properties from pristine conditions

Given diverse responses of sediments to HCl concentrations and acid fumigation, it is reasonable to assume that all pretreatment conditions would have resulted in ~~noticeable~~ traceable deviation of sample properties away from pristine conditions held by unprocessed raw materials. This is verified and examined by comparing ~~To verify and examine the extent of deviations, we compared~~ RPO thermograms between acidified (i.e., rinsing ~~versus~~ , fumigation) and unacidified subsamples. Due to the influence of IC in raw materials, thermograms of both processed and raw sediments were first normalized to back-calculated TOC content of each specific sample. As organic carbon contents of raw subsamples cannot be directly estimated, we used back-calculated TOC of ~~fume II~~fumigated subsamples, which minimize OC loss, to approximate those of raw subsamples. Former studies suggested that IC decomposition normally commences at ~~about~~ ~ 500 °C or higher (Capel et al., 2006; Hemingway et al., 2017a). Thus, we only focus on thermographic segments evolved under 450 °C, below which IC decomposition and consequential CO_2 production are considered to be negligible. Accordingly, we assume that any apparent inconformity of thermograms is ascribed to OC decomposition or alteration.

When thermograms are overlain together, acid rinsed subsamples, with the exception of ~~AREX R7~~Sed2, are, on average, more ~~proximal~~similar to pristine conditions (Fig. ~~5~~4). It is noteworthy that the instantaneous CO_2 ~~magnitude~~ concentrations of raw material ~~thermograms~~ may be overestimated, due to the potential decomposition of some carbonate minerals at lower temperatures (Hazra et al., 2022; Sebag et al., 2018) and/or OC loss during acid fumigation. Low-temperature-prone carbonates may reasonably explain the abnormality of ~~AREX R7~~Sed2, of which the raw material features relatively low μ_E (182.48 kJ mol^{-1}; not shown) and T_{max} value (Supplementary file Fig. S6~~5~~). Accordingly, we are confident to conclude that acid rinsing is more conducive to maintaining sediment pristine conditions, producing reliable and ~~consistent~~ unbiased thermochemical results.

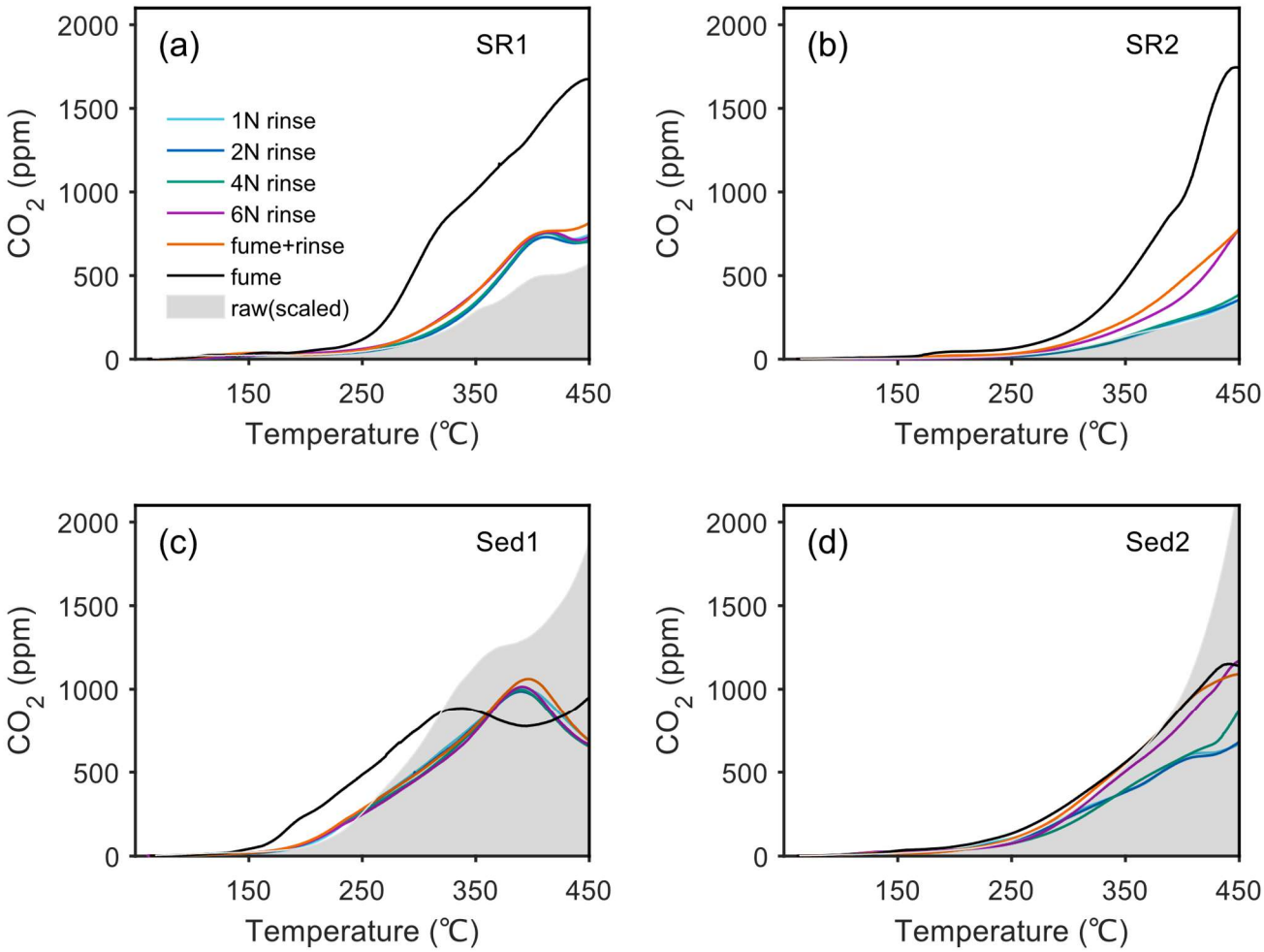

Fig ~~5~~4: Evaluation of the ~~proximity~~ similarity to the natural pristine states of subsamples acidified by different methods. **(a)**, **(b)**, **(c)**, and **(d)** are subsamples of ~~1207-GR-11~~SR1, ~~MS05-135~~SR2, ~~CJK-A6-3~~Sed1, and ~~AREX-R7~~Sed2, respectively. Each curve represents the thermogram of a subsample acidified by corresponding procedure~~s~~. The grey area in each subgraph is the thermogram of the raw (unacidified) aliquot after normalization to OC contents.

4 Conclusion and recommendations

~~In t~~This study~~,~~ ~~we applied different acidification methods and~~systematically evaluated how decarbonation pretreatments influence ~~RPO~~ramped-temperature pyrolysis/oxidation (RPO) ~~analyses~~measurements of ~~with~~sedimentary OC~~four representative samples to systematically evaluated the effects of twelve different acidification pretreatments on decarbonation using four representative samples~~RPO results. We ~~Our~~ RPO ~~results~~ demonstrate that ~~the choice between~~ both acid rinsing (particularly~~and~~ acid concentration) and fumigation~~, as well as HCl concentrations during acid rinsing,~~ significantly alter ~~are~~

two critical factors influencing bulk OC and thermochemical properties, . Hwith higher HCl acid concentrations led topromoting greater OC loss, likely due to mineral dissolution by concentrated HCl, which alters, modifying organo-mineral interaction and leachinges soluble OC fractions. Crucially, RPO profiles exhibited remarkable methodological differences method-dependent disparities, where acid fumigation introducesd artifacts through Furthermore, significant differences in thermochemicalRPO results were observed between acid rinsing and fumigation. Through simulation experiments with an in-house standard, we attribute these differences to corrosive impacts from $CaCl_2$ decomposition and alterations of thermochemical properties by strong acid vapor exposure, while controlled acid rinsing with diluted HCl better preservesd native natural OC characteristics. These findings highlight that pretreatment selection directly impactsipacts the interpretation of thermal degradation characteristicsbehavior in sedimentary systems. during acid fumigation.

Based on these findings, we recommendFor reliable RPO analysis, we advocate suggest using diluted HCl rinsing with moderate reaction times (~12h) for acid rinsing, as it minimizesthe optimal balance between perturbation to the pristine conditions of raw samplesinorganic carbon removal and minimal. Further studies that directly analyze soluble OC in the supernatant after acidification can accurately discern the compounds and provide supportive evidence of this study. Fourier transform infrared spectroscopy (FTIR) and other analytical methods can be informative as well to reveal the changes in OC composition and organo-mineral associations in sediments (Kleber et al., 2015).

Given results from this study, we propose the following suggestions for future decarbonation pretreatments before RPO and other analyses. First, acid fumigation of sediments in silver capsules is preferred for the measurements of bulk OC and $\delta^{13}C$ values. However, acid fumigation is not applicable to samples containing a considerable content of carbonates as it removes IC incompletely. Acid rinsing with low concentrations of HCl induces minimal OC alteration to organo-mineral interactions and is the ideal decarbonation pretreatment preceding thermochemical (e.g., RPO, Rock-Eval, thermogravimetric analysis), spectral (e.g., Raman) and molecular (e.g., biomarker) analyses. Other secondary factors (e.g., reaction time) likely have limited impacts on RPO results but may introduce greater biases in bulk carbon measurement. In additionNonetheless, to completely remove IC and to minimize OC loss, moderate reaction time (~12 h or overnight) and freeze-drying are recommended. However, it should be noticed that fFreeze-drying remains effective but requires ier may be an underlyingadd organic contamination without thoroughunless equipment is cleanstrict contamination controling (Jiang et al., 2023). Furthermore, operations to accelerate the decarbonation process, likeWhile heating accelerates decarbonation and sonication (not verified in this study), seemingly do not produce significant deviations. However,it should be avoided for organic-rich (e.g., protein-rich) samplessediments to prevent hydrolytic OC loss and , this may not be the case as heating may accelerate the hydrolysis of proteins and cause significant leaching of soluble OC. Further studies should incorporate supernatant analysis of acid-that directly analyze soluble OC in the supernatant after acidification can accurately discern the compounds and provide supportive evidence of this study.and complementary techniques like FourierFFfourier transform infrared spectroscopy (FTIR) and other analytical methods can be informative as well to reveal the changes in OC composition and organo-mineral associations in sedimentsto fully characterize pretreatment impacts (Kleber et al., 2015). BesidesFinally, our studyOverall,

~~T~~this work establishes that RPO~~PRO~~, when paired with appropriate sample preparation, can resolve ~~suggests that thermochemical analysis can be a powerful way to disentangle~~ subtle OC properties ~~unresolvable~~ obscured by bulk analytical approaches~~, provided method-induced biases are carefully mitigated~~~~parameters~~.

Data availability

All data needed to evaluate the conclusions is involved in this paper and the supplementary file. The RPO dataset of this study can be accessible through DOI: 10.5281/zenodo.14825000 (He et al., 2025).

Author contribution

S.H. and X.C. designed the study; S.H. and H.Y. conducted the experiments; X.C. secured fundings; S.H. drafted the manuscript with contributions from all co-authors.

Competing interests

The authors declare no conflict of interest.

Acknowledgements

This work was financially supported by Shanghai "Phosphor" Science Foundation (No. 24QA2704000) and National Natural Science Foundation of China (No. 42273075). We would like to thank Dr. Jordon D. Hemingway for allowing access to the corresponding Python package, Dr. Katarzyna Koziorowska-Makuch for the AREX R7 sample, and Wanhua Huang for the CJK A6-3 sample.

References

Bao, R., Strasser, M., McNichol, A. P., Haghipour, N., McIntyre, C., Wefer, G., and Eglinton, T. I.: Tectonically-triggered sediment and carbon export to the Hadal zone, Nat. Commun., 9, 121, https://doi.org/10.1038/s41467-017-02504-1, 2018.

Bao, R., McNichol, A. P., Hemingway, J. D., Lardie Gaylord, M. C., and Eglinton, T. I.: Influence of Different Acid Treatments on the Radiocarbon Content Spectrum of Sedimentary Organic Matter Determined by RPO/Accelerator Mass Spectrometry, Radiocarbon, 61, 395–413, https://doi.org/10.1017/RDC.2018.125, 2019.

Blattmann, T. M., Liu, Z., Zhang, Y., Zhao, Y., Haghipour, N., Montluçon, D. B., Plötze, M., and Eglinton, T. I.: Mineralogical control on the fate of continentally derived organic matter in the ocean, Science, 366, 742–745, https://doi.org/10.1126/science.aax5345, 2019.

525 Brodie, C. R., Leng, M. J., Casford, J. S. L., Kendrick, C. P., Lloyd, J. M., Yongqiang, Z., and Bird, M. I.: Evidence for bias in C and N concentrations and δ13C composition of terrestrial and aquatic organic materials due to pre-analysis acid preparation methods, Chem. Geol., 282, 67–83, https://doi.org/10.1016/j.chemgeo.2011.01.007, 2011.

Burdige, D. J.: Preservation of Organic Matter in Marine Sediments: Controls, Mechanisms, and an Imbalance in Sediment Organic Carbon Budgets?, Chem. Rev., 107, 467–485, https://doi.org/10.1021/cr050347q, 2007.

530 Capel, E. L., De La Rosa Arranz, J. M., González-Vila, F. J., González-Perez, J. A., and Manning, D. A. C.: Elucidation of different forms of organic carbon in marine sediments from the Atlantic coast of Spain using thermal analysis coupled to isotope ratio and quadrupole mass spectrometry, Org. Geochem., 37, 1983–1994, https://doi.org/10.1016/j.orggeochem.2006.07.025, 2006.

Craddock, P. R., Bake, K. D., and Pomerantz, A. E.: Chemical, Molecular, and Microstructural Evolution of Kerogen during
535 Thermal Maturation: Case Study from the Woodford Shale of Oklahoma, Energy Fuels, 32, 4859–4872, https://doi.org/10.1021/acs.energyfuels.8b00189, 2018.

Cui, X., Mucci, A., Bianchi, T. S., He, D., Vaughn, D., Williams, E. K., Wang, C., Smeaton, C., Koziorowska-Makuch, K., Faust, J. C., Plante, A. F., and Rosenheim, B. E.: Global fjords as transitory reservoirs of labile organic carbon modulated by organo-mineral interactions, Sci. Adv., 8, eadd0610, https://doi.org/10.1126/sciadv.add0610, 2022.

540 De Lecea, A. M., Smit, A. J., and Fennessy, S. T.: The effects of freeze/thaw periods and drying methods on isotopic and elemental carbon and nitrogen in marine organisms, raising questions on sample preparation, Rapid Commun. Mass Spectrom., 25, 3640–3649, https://doi.org/10.1002/rcm.5265, 2011.

Feng, X., Simpson, A. J., and Simpson, M. J.: Chemical and mineralogical controls on humic acid sorption to clay mineral surfaces, Org. Geochem., 36, 1553–1566, https://doi.org/10.1016/j.orggeochem.2005.06.008, 2005.

545 Fernandez, A. and Borrok, D. M.: Fractionation of Cu, Fe, and Zn isotopes during the oxidative weathering of sulfide-rich rocks, Chem. Geol., 264, 1–12, https://doi.org/10.1016/j.chemgeo.2009.01.024, 2009.

Fujisaki, W., Matsui, Y., Ueda, H., Sawaki, Y., Suzuki, K., and Maruoka, T.: Pre-treatment Methods for Accurate Determination of Total Nitrogen and Organic Carbon Contents and their Stable Isotopic Compositions: Re-evaluation from Geological Reference Materials, Geostand. Geoanalytical Res., 46, 5–19, https://doi.org/10.1111/ggr.12410, 2022.

550 Galy, V., Bouchez, J., and France-Lanord, C.: Determination of Total Organic Carbon Content and δ^{13} C in Carbonate-Rich Detrital Sediments, Geostand. Geoanalytical Res., 31, 199–207, https://doi.org/10.1111/j.1751-908X.2007.00864.x, 2007.

Harris, D., Horwáth, W. R., and Van Kessel, C.: Acid fumigation of soils to remove carbonates prior to total organic carbon or CARBON-13 isotopic analysis, Soil Sci. Soc. Am. J., 65, 1853–1856, https://doi.org/10.2136/sssaj2001.1853, 2001.

Hazra, B., Katz, B. J., Singh, D. P., and Singh, P. K.: Impact of siderite on Rock-Eval S3 and oxygen index, Mar. Pet. Geol.,
555 143, 105804, https://doi.org/10.1016/j.marpetgeo.2022.105804, 2022.

He, S., Yang, H., and Cui, X.: Dataset for acidification impacts on sediment decarbonation (V1.0), https://doi.org/10.5281/ZENODO.14825000, 2025.

Hedges, J. I. and Stern, J. H.: Carbon and nitrogen determinations of carbonate-containing solids1, Limnol. Oceanogr., 29, 657–663, https://doi.org/10.4319/lo.1984.29.3.0657, 1984.

Hemingway, J. D.: rampedpyrox: Open-source tools for thermoanalytical data analysis, 2016-, https://doi.org/10.5281/zenodo.839815, 2017.

Hemingway, J. D., Rothman, D. H., Rosengard, S. Z., and Galy, V. V.: Technical note: An inverse method to relate organic carbon reactivity to isotope composition from serial oxidation, Biogeosciences, 14, 5099–5114, https://doi.org/10.5194/bg-14-5099-2017, 2017a.

Hemingway, J. D., Galy, V. V., Gagnon, A. R., Grant, K. E., Rosengard, S. Z., Soulet, G., Zigah, P. K., and McNichol, A. P.: Assessing the Blank Carbon Contribution, Isotope Mass Balance, and Kinetic Isotope Fractionation of the Ramped Pyrolysis/Oxidation Instrument at NOSAMS, Radiocarbon, 59, 179–193, https://doi.org/10.1017/RDC.2017.3, 2017b.

Hemingway, J. D., Hilton, R. G., Hovius, N., Eglinton, T. I., Haghipour, N., Wacker, L., Chen, M.-C., and Galy, V. V.: Microbial oxidation of lithospheric organic carbon in rapidly eroding tropical mountain soils, Science, 360, 209–212, https://doi.org/10.1126/science.aao6463, 2018.

Hemingway, J. D., Rothman, D. H., Grant, K. E., Rosengard, S. Z., Eglinton, T. I., Derry, L. A., and Galy, V. V.: Mineral protection regulates long-term global preservation of natural organic carbon, Nature, 570, 228–231, https://doi.org/10.1038/s41586-019-1280-6, 2019.

Huang, W., Yang, H., He, S., Zhao, B., and Cui, X.: Thermochemical decomposition reveals distinct variability of sedimentary organic carbon reactivity along the Yangtze River estuary-shelf continuum, Mar. Chem., 257, 104326, https://doi.org/10.1016/j.marchem.2023.104326, 2023.

Ingalls, A. E., Aller, R. C., Lee, C., and Wakeham, S. G.: Organic matter diagenesis in shallow water carbonate sediments, Geochim. Cosmochim. Acta, 68, 4363–4379, https://doi.org/10.1016/j.gca.2004.01.002, 2004.

Jiang, C., Robinson, R., Vandenberg, R., Milovic, M., and Neville, L.: Oil contamination of sediments by freeze-drying versus air-drying for organic geochemical analysis, Environ. Geochem. Health, 45, 5799–5811, https://doi.org/10.1007/s10653-023-01594-9, 2023.

Keil, R. G. and Mayer, L. M.: Mineral Matrices and Organic Matter, in: Treatise on Geochemistry, Elsevier, 337–359, https://doi.org/10.1016/B978-0-08-095975-7.01024-X, 2014.

Kennedy, M. J., Pevear, D. R., and Hill, R. J.: Mineral Surface Control of Organic Carbon in Black Shale, Science, 295, 657–660, https://doi.org/10.1126/science.1066611, 2002.

Kennedy, M. J., Löhr, S. C., Fraser, S. A., and Baruch, E. T.: Direct evidence for organic carbon preservation as clay-organic nanocomposites in a Devonian black shale; from deposition to diagenesis, Earth Planet. Sci. Lett., 388, 59–70, https://doi.org/10.1016/j.epsl.2013.11.044, 2014.

Kim, M., Lee, W., Suresh Kumar, K., Shin, K., Robarge, W., Kim, M., and Lee, S. R.: Effects of HCl pretreatment, drying, and storage on the stable isotope ratios of soil and sediment samples, Rapid Commun. Mass Spectrom., 30, 1567–1575, https://doi.org/10.1002/rcm.7600, 2016.

Kleber, M., Eusterhues, K., Keiluweit, M., Mikutta, C., Mikutta, R., and Nico, P. S.: Mineral–Organic Associations: Formation, Properties, and Relevance in Soil Environments, in: Advances in Agronomy, vol. 130, Elsevier, 1–140, https://doi.org/10.1016/bs.agron.2014.10.005, 2015.

595 Komada, T., Anderson, M. R., and Dorfmeier, C. L.: Carbonate removal from coastal sediments for the determination of organic carbon and its isotopic signatures, δ^{13} C and Δ^{14} C: comparison of fumigation and direct acidification by hydrochloric acid, Limnol. Oceanogr. Methods, 6, 254–262, https://doi.org/10.4319/lom.2008.6.254, 2008.

Kumar, P., Jasra, R. V., and Bhat, T. S. G.: Evolution of Porosity and Surface Acidity in Montmorillonite Clay on Acid Activation, Ind. Eng. Chem. Res., 34, 1440–1448, https://doi.org/10.1021/ie00043a053, 1995.

600 Lalonde, K., Mucci, A., Ouellet, A., and Gélinas, Y.: Preservation of organic matter in sediments promoted by iron, Nature, 483, 198–200, https://doi.org/10.1038/nature10855, 2012.

Lohse, L., Kloosterhuis, R. T., De Stigter, H. C., Helder, W., Van Raaphorst, W., and Van Weering, T. C. E.: Carbonate removal by acidification causes loss of nitrogenous compounds in continental margin sediments, Mar. Chem., 69, 193–201, https://doi.org/10.1016/S0304-4203(99)00105-X, 2000.

605 Mackey, D. J. and Zirino, A.: Comments on trace metal speciation in seawater or do "onions" grow in the sea?, Anal. Chim. Acta, 284, 635–647, https://doi.org/10.1016/0003-2670(94)85068-2, 1994.

Maier, K. L., Ginnane, C. E., Naeher, S., Turnbull, J. C., Nodder, S. D., Howarth, J., Bury, S. J., Hilton, R. G., and Hillman, J. I.: Earthquake-triggered submarine canyon flushing transfers young terrestrial and marine organic carbon into the deep sea, Earth Planet. Sci. Lett., 654, 119241, https://doi.org/10.1016/j.epsl.2025.119241, 2025.

610 Mayer, L. M.: Relationships between mineral surfaces and organic carbon concentrations in soils and sediments, Chem. Geol., 114, 347–363, https://doi.org/10.1016/0009-2541(94)90063-9, 1994a.

Mayer, L. M.: Surface area control of organic carbon accumulation in continental shelf sediments, Geochim. Cosmochim. Acta, 58, 1271–1284, https://doi.org/10.1016/0016-7037(94)90381-6, 1994b.

McClymont, E. L., Martínez-Garcia, A., and Rosell-Melé, A.: Benefits of freeze-drying sediments for the analysis of total
615 chlorins and alkenone concentrations in marine sediments, Org. Geochem., 38, 1002–1007, https://doi.org/10.1016/j.orggeochem.2007.01.006, 2007.

Pasquier, V., Sansjofre, P., Lebeau, O., Liorzou, C., and Rabineau, M.: Acid digestion on river influenced shelf sediment organic matter: Carbon and nitrogen contents and isotopic ratios, Rapid Commun. Mass Spectrom., 32, 86–92, https://doi.org/10.1002/rcm.8014, 2018.

620 Plante, A. F., Beaupré, S. R., Roberts, M. L., and Baisden, T.: Distribution of Radiocarbon Ages in Soil Organic Matter by Thermal Fractionation, Radiocarbon, 55, 1077–1083, https://doi.org/10.1017/S0033822200058215, 2013.

Rongemaille, E., Bayon, G., Pierre, C., Bollinger, C., Chu, N. C., Fouquet, Y., Riboulot, V., and Voisset, M.: Rare earth elements in cold seep carbonates from the Niger delta, Chem. Geol., 286, 196–206, https://doi.org/10.1016/j.chemgeo.2011.05.001, 2011.

625 Rosenheim, B. E., Day, M. B., Domack, E., Schrum, H., Benthien, A., and Hayes, J. M.: Antarctic sediment chronology by programmed-temperature pyrolysis: Methodology and data treatment, Geochem. Geophys. Geosystems, 9, 2007GC001816, https://doi.org/10.1029/2007GC001816, 2008.

Rosenheim, B. E., Santoro, J. A., Gunter, M., and Domack, E. W.: Improving Antarctic Sediment^{14} C Dating Using Ramped Pyrolysis: An Example from the Hugo Island Trough, Radiocarbon, 55, 115–126,
630 https://doi.org/10.2458/azu_js_rc.v55i1.16234, 2013.

Rowley, M. C., Grand, S., and Verrecchia, É. P.: Calcium-mediated stabilisation of soil organic carbon, Biogeochemistry, 137, 27–49, https://doi.org/10.1007/s10533-017-0410-1, 2018.

Schlacher, T. A. and Connolly, R. M.: Effects of acid treatment on carbon and nitrogen stable isotope ratios in ecological samples: a review and synthesis, Methods Ecol. Evol., 5, 541–550, https://doi.org/10.1111/2041-210X.12183, 2014.

Sebag, D., Garcin, Y., Adatte, T., Deschamps, P., Ménot, G., and Verrecchia, E. P.: Correction for the siderite effect on Rock-Eval parameters: Application to the sediments of Lake Barombi (southwest Cameroon), Org. Geochem., 123, 126–135, https://doi.org/10.1016/j.orggeochem.2018.05.010, 2018.

Serrano, O., Mazarrasa, I., Fourqurean, J. W., Serrano, E., Baldock, J., and Sanderman, J.: Flaws in the methodologies for organic carbon analysis in seagrass blue carbon soils, Limnol. Oceanogr. Methods, 21, 814–827, https://doi.org/10.1002/lom3.10583, 2023.

Sowers, T. D., Stuckey, J. W., and Sparks, D. L.: The synergistic effect of calcium on organic carbon sequestration to ferrihydrite, Geochem. Trans., 19, https://doi.org/10.1186/s12932-018-0049-4, 2018.

Stoner, S. W., Schrumpf, M., Hoyt, A., Sierra, C. A., Doetterl, S., Galy, V., and Trumbore, S.: How well does ramped thermal oxidation quantify the age distribution of soil carbon? Assessing thermal stability of physically and chemically fractionated soil organic matter, Biogeosciences, 20, 3151–3163, https://doi.org/10.5194/bg-20-3151-2023, 2023.

Summons, R. E., Bird, L. R., Gillespie, A. L., Pruss, S. B., Roberts, M., and Sessions, A. L.: Lipid biomarkers in ooids from different locations and ages: evidence for a common bacterial flora, Geobiology, 11, 420–436, https://doi.org/10.1111/gbi.12047, 2013.

Venturelli, R. A., Siegfried, M. R., Roush, K. A., Li, W., Burnett, J., Zook, R., Fricker, H. A., Priscu, J. C., Leventer, A., and Rosenheim, B. E.: Mid-Holocene Grounding Line Retreat and Readvance at Whillans Ice Stream, West Antarctica, Geophys. Res. Lett., 47, e2020GL088476, https://doi.org/10.1029/2020GL088476, 2020.

Vogel, C., Mueller, C. W., Höschen, C., Buegger, F., Heister, K., Schulz, S., Schloter, M., and Kögel-Knabner, I.: Submicron structures provide preferential spots for carbon and nitrogen sequestration in soils, Nat. Commun., 5, 2947, https://doi.org/10.1038/ncomms3947, 2014.

Williams, E. K., Rosenheim, B. E., McNichol, A. P., and Masiello, C. A.: Charring and non-additive chemical reactions during ramped pyrolysis: Applications to the characterization of sedimentary and soil organic material, Org. Geochem., 77, 106–114, https://doi.org/10.1016/j.orggeochem.2014.10.006, 2014.

Wu, Y., Zhang, Q., Zhuo, J., Dong, S., and Yao, Q.: Influence of calcium chloride on the fine particulate matter formation during coal pyrolysis, Fuel, 355, 129480, https://doi.org/10.1016/j.fuel.2023.129480, 2024.

Yamamuro, M. and Kayanne, H.: Rapid direct determination of organic carbon and nitrogen in carbonate-bearing sediments with a Yanaco MT-5 CHN analyzer, Limnol. Oceanogr., 40, 1001–1005, https://doi.org/10.4319/lo.1995.40.5.1001, 1995.

Yang, H., Ma, J., He, S., Wang, J., Sun, Y., and Cui, X.: Resistant degradation of petrogenic organic carbon in the weathering of calcareous rocks, Glob. Planet. Change, 246, 104727, https://doi.org/10.1016/j.gloplacha.2025.104727, 2025.

Zeller, M. A., Van Dam, B. R., Lopes, C., and Kominoski, J. S.: Carbonate-Associated Organic Matter Is a Detectable Dissolved Organic Matter Source in a Subtropical Seagrass Meadow, Front. Mar. Sci., 7, 580284, https://doi.org/10.3389/fmars.2020.580284, 2020.

Zeller, M. A., Van Dam, B. R., Lopes, C., McKenna, A. M., Osburn, C. L., Fourqurean, J. W., Kominoski, J. S., and Böttcher, M. E.: The unique biogeochemical role of carbonate-associated organic matter in a subtropical seagrass meadow, Commun. Earth Environ., 5, 681, https://doi.org/10.1038/s43247-024-01832-7, 2024.

Zhang, X., Bianchi, T. S., Cui, X., Rosenheim, B. E., Ping, C., Hanna, A. J. M., Kanevskiy, M., Schreiner, K. M., and Allison, M. A.: Permafrost Organic Carbon Mobilization From the Watershed to the Colville River Delta: Evidence From ^{14}C Ramped Pyrolysis and Lignin Biomarkers, Geophys. Res. Lett., 44, https://doi.org/10.1002/2017GL075543, 2017.

Zhang, Y., Galy, V., Yu, M., Zhang, H., and Zhao, M.: Terrestrial organic carbon age and reactivity in the Yellow River fueling efficient preservation in marine sediments, Earth Planet. Sci. Lett., 585, 117515, https://doi.org/10.1016/j.epsl.2022.117515, 2022.